SLAC-PUB-5981
January 1993
T

The Heavy Quark Self-Energy in Nonrelativistic Lattice QCD

Colin J. Morningstar
Stanford Linear Accelerator Center
Stanford University, Stanford, California 94309

The heavy quark self-energy in nonrelativistic lattice QCD is calculated to $O(\alpha_s)$ in perturbation theory. An action which includes all spin-independent relativistic corrections to order v^2, where v is the typical heavy quark velocity, and all spin-dependent corrections to order v^4 is used. The standard Wilson action and an improved multi-plaquette action are used for the gluons. Results for the mass renormalization, wavefunction renormalization, and energy shift are given; tadpole contributions are found to be large. A tadpole improvement scheme in which all link variables are rescaled by a mean-field factor is also studied. The effectiveness of this scheme in offsetting the large tadpole contributions to the heavy quark renormalization parameters is demonstrated.

Submitted to *Physical Review D*

• Work supported by the Department of Energy, Contract No. DE-AC03-76SF00515 and by the Natural Sciences and Engineering Research Council of Canada.

I. INTRODUCTION

Quantum chromodynamics (QCD) has been very successful in describing the high-energy interactions of quarks and gluons; however, despite nearly two decades of lattice simulations, attempts to extract from the theory reliable quantitative information on the low-energy properties of hadrons have not been fully successful.

Recently, a new approach has been suggested [1] which advocates combining effective field theory and lattice techniques to study hadrons composed entirely of heavy quarks. There are many good reasons for doing this. Such hadrons are the simplest to analyze since the quarks are nonrelativistic. Simulations which use a nonrelativistic QCD (NRQCD) action instead of the usual Dirac action are far more efficient since the heavy-quark propagator can be computed as an initial-value problem in a single sweep through the lattice. The Dirac propagator is a boundary-value problem which must be solved iteratively using many sweeps. Also, the fermion doubling problem does not occur in the nonrelativistic theory. Heavy quarkonia, such as the ψ and Υ mesons, are small so that lattice volumes presently used are sufficiently large, and their properties are fairly insensitive to both light-quark vacuum polarization effects [2], which are very expensive to simulate, and to heavy-quark vacuum polarization. Simulations of heavy quarkonia do not suffer from a rapid reduction in the signal-to-noise ratio which is a serious shortcoming of the static approximation used to study heavy-light systems, such as the D and B mesons. Quarkonia are well understood; this makes possible good control of systematic errors which is necessary for precise tests of QCD. Furthermore, an abundance of experimental data on quarkonium states is available to which the simulation results, such as level splittings, decay constants, and wavefunctions, may be compared.

NRQCD is an effective cutoff field theory constructed from a set of nonrenormalizable interactions specified solely by the symmetries of QCD, the chosen regulator, locality, and the accuracy desired. It is essentially a low-energy expansion of the Dirac theory in terms of the expectation value v of the heavy quark velocity in a typical heavy quark hadron. An action which includes all spin-independent relativistic interactions suppressed by v^2 relative to the leading terms and all spin-dependent corrections up to order v^4 has previously been formulated using a lattice regularization scheme [2] and is here referred to as lattice NRQCD. To fully define lattice NRQCD, the coupling coefficients of the interactions appearing in the action must be specified. These are process and momentum independent and are uniquely determined (for a given regulator) by requiring that lattice NRQCD exactly reproduces the results of continuum QCD at low energies.

Since the role of these couplings is to absorb the relativistic effects arising from highly-ultraviolet QCD processes, one expects that they may be computed to a good approximation using perturbation theory, provided the quark mass M is large enough. The simplest way to proceed is to evaluate various scattering amplitudes both in QCD and lattice NRQCD and adjust the couplings until these amplitudes agree to the desired order in v and the QCD coupling g. In this way, one obtains coupling

coefficients which are power series in $g^2(\Lambda)$, where Λ is the cutoff of the effective theory. The cutoff Λ must be large enough so that $O(g^2(\Lambda))$ corrections to the effective couplings are small, making a perturbative analysis meaningful. However, power-law divergences generally occur, producing terms such as $g^2(\Lambda)\Lambda/M$ which render perturbation theory useless if Λ is made too large.

In this paper, the lowest-order corrections to the heavy quark self-energy in lattice NRQCD are calculated using weak-coupling perturbation theory. The action formulated in Ref. [2] which includes spin effects is used. Similar to an earlier study [3], the mass and wavefunction renormalization parameters required to match continuum QCD are obtained, as well as a necessary overall energy shift. Lattice NRQCD is briefly described in Section II. The Feynman rules are derived in Section III and the self-energy calculations are presented and discussed in Section IV. A tadpole improvement scheme in which all link variables are rescaled by a mean-field factor (link variable renormalization) is also studied. Taking into account the mean-field corrections introduced by this scheme, the coefficients of g^2 in the heavy quark renormalization parameters are found to be small. Section V offers conclusions.

II. LATTICE NRQCD

Standard renormalization group techniques are used to formulate the NRQCD action. First, since the physics of heavy quark systems is dominated by momenta $p \sim Mv \ll M$, where M is the heavy quark mass, an ultraviolet cutoff $\Lambda \sim M$ is introduced. The Dirac action can then be replaced by a nonrelativistic Schrödinger action in which the quark and antiquark degrees of freedom essentially decouple. However, new local interactions must be added in order to compensate for the loss of the discarded relativistic states. Power counting rules [2] are used to classify these interactions according to their estimated magnitude in a typical quarkonium state as measured in terms of v. Equipped with these rules, the interaction terms which contribute to quarkonia physics up to some given order in v may then be enumerated. The couplings associated with these interactions are determined by requiring agreement between the physical results of NRQCD and those of full QCD through the specified order in the quark velocity. When formulated on a lattice, NRQCD becomes a particularly powerful tool for studying heavy quark systems.

In lattice simulations, Euclidean space correlation functions are computed. These may be obtained from the Minkowski theory by Wick rotating the contour integral of the Lagrangian over time from the real axis to the imaginary axis in a clockwise manner. Also, the path integration over the scalar potential must be similarly Wick rotated at each point in space-time. Then by defining $x^4 = ix^0$, $x_4 = -ix_0$, $A^4 = iA^0$, and $A_4 = -iA_0$, one can again work with real quantities. The spatial components of all four-vectors remain unchanged. The path integral weight $\exp(iS)$ becomes $\exp(-S_E)$, where S_E is called the Euclidean action. Wick rotation transforms the Minkowski metric tensor $g_{\mu\nu} = \mathrm{diag}(1,-1,-1,-1)$ into the negative of the identity

matrix, so that in Euclidean space, raising or lowering any index introduces a sign change.

In lattice NRQCD, the quark fields are defined on the sites of a four-dimensional hypercubic lattice with spacing a, while the gauge-field degrees of freedom reside on the links between the sites. With each link originating at a site x and terminating at a site $x + a\hat{e}_\mu$ is associated a link variable $U_\mu(x)$, which is a lattice version of the parallel transport matrix between sites and is an element of the Lie group associated with the gauge invariance of the theory. A lattice gluon field $A_\mu(x) = \sum_{b=1}^{8} A_\mu^b(x) T^b$ may be defined in terms of the link variables using

$$U_\mu(x) = \exp\left[iagA_\mu(x + \frac{a}{2}\hat{e}_\mu)\right], \tag{1}$$

where g is the coupling constant of the theory and $(\hat{e}_\mu)^\alpha = \delta_\mu^\alpha$. This definition is convenient since it is simple and satisfies $U_\mu^\dagger(x) = U_{-\mu}(x + a\hat{e}_\mu)$. The SU(3) generators T^b are Hermitian, traceless, and satisfy $\mathrm{Tr}(T^a T^b) = \frac{1}{2}\delta^{ab}$ and $[T^a, T^b] = if^{abc}T^c$, where f^{abc} are the real, fully antisymmetric structure constants. Of course, the field $A_\mu(x)$ is not identical to the gluon field of the continuum theory. Let $G_\mu(x)$ represent the gluon field defined in the continuum theory. Under a local gauge transformation $S(x)$, $G_\mu(x) \longrightarrow S(x)G_\mu(x)S^\dagger(x) - (i/g)S(x)\partial_\mu S^\dagger(x)$. The field $A_\mu(x)$ does not transform in this way; rather, it transforms in a very complicated manner in order that the link variable transforms under a local gauge transformation according to $U_\mu(x) \longrightarrow S(x)U_\mu(x)S^\dagger(x + a\hat{e}_\mu)$.

In Minkowski space, the chromoelectric and chromomagnetic fields are usually defined in terms of the field strength tensor in the following manner: $E_{(M)}^k(x) = F^{k0}(x) = F_{0k}(x)$, and $B^k(x) = -\frac{1}{2}\epsilon_{klm}F^{lm}(x)$, where $\epsilon_{123} = 1$. In Euclidean space, the magnetic field is unchanged. The electric field in Euclidean space is here defined by $E^k(x) = F^{k4}(x) = -F_{4k}(x)$, so that $E_{(M)}^k = -iE^k$. The Hermitian and traceless field strength tensor is best represented [4] by cloverleaf operators defined at the sites of the lattice:

$$F_{\mu\nu}(x) = \mathcal{F}_{\mu\nu}(x) - \frac{1}{3}\mathrm{Tr}\mathcal{F}_{\mu\nu}(x), \tag{2}$$

$$\mathcal{F}_{\mu\nu}(x) = \frac{-i}{2a^2 g}\left(\Omega_{\mu\nu}(x) - \Omega_{\mu\nu}^\dagger(x)\right), \tag{3}$$

$$\Omega_{\mu\nu}(x) = \frac{1}{4}\sum_{\{(\alpha,\beta)\}_{\mu\nu}} U_\alpha(x)U_\beta(x + a\hat{e}_\alpha)U_{-\alpha}(x + a\hat{e}_\alpha + a\hat{e}_\beta)U_{-\beta}(x + a\hat{e}_\beta), \tag{4}$$

with $\{(\alpha,\beta)\}_{\mu\nu} = \{(\mu,\nu),(\nu,-\mu),(-\mu,-\nu),(-\nu,\mu)\}$ for $\mu \neq \nu$. This representation is chosen since it transforms as the $(1,0) \oplus (0,1)$ six-dimensional reducible representation of the hypercubic group, similar to the continuum case.

Covariant derivatives are replaced by forward, backward, or symmetric differences on the lattice:

$$a^5\Delta_\mu^{(+)}(y;x) = U_\mu(y)\hat{\delta}^{(4)}(x, y + a\hat{e}_\mu) - \hat{\delta}^{(4)}(x, y), \tag{5}$$

$$a^5\Delta_\mu^{(-)}(y;x) = \hat{\delta}^{(4)}(x, y) - U_\mu^\dagger(x)\hat{\delta}^{(4)}(x, y - a\hat{e}_\mu), \tag{6}$$

$$\Delta^{(\pm)} = \frac{1}{2}(\Delta^{(+)} + \Delta^{(-)}), \tag{7}$$

where $\hat{\delta}^{(4)}(x, y)$ denotes a four-dimensional Kronecker δ-function. For example,

$$\sum_x a^5\Delta_\mu^{(+)}(y;x)\psi(x) = U_\mu(y)\psi(y+a\hat{e}_\mu) - \psi(y). \tag{8}$$

Also, the Laplacian becomes

$$\mathbf{\Delta}^{(2)} = \sum_{k=1}^{3} \Delta_k^{(+)}\Delta_k^{(-)} = \sum_{k=1}^{3} \Delta_k^{(-)}\Delta_k^{(+)}. \tag{9}$$

The finite lattice spacing introduces systematic errors into NRQCD which can be reduced by the addition of new interactions to the action. At tree level, this is most easily accomplished by improving the components comprising the lattice action so that they more accurately reproduce the effects of their continuum counterparts. An improved difference operator which reproduces the behavior of the continuum covariant derivative through order a^4 is given by

$$\tilde{\Delta}_k^{(\pm)} = \Delta_k^{(\pm)} - \frac{a^2}{6}\Delta_k^{(+)}\Delta_k^{(\pm)}\Delta_k^{(-)}. \tag{10}$$

An improved lattice Laplacian is

$$\tilde{\mathbf{\Delta}}^{(2)} = \mathbf{\Delta}^{(2)} - \frac{a^2}{12}\sum_{k=1}^{3}\left(\Delta_k^{(+)}\Delta_k^{(-)}\right)^2. \tag{11}$$

Lastly, an improved cloverleaf field strength tensor may be defined by

$$\tilde{F}_{\mu\nu}(x) = \frac{5}{3}F_{\mu\nu}(x) - \frac{1}{6}\left[U_\mu(x)F_{\mu\nu}(x + a\hat{e}_\mu)U_\mu^\dagger(x) + U_\mu^\dagger(x - a\hat{e}_\mu)F_{\mu\nu}(x - a\hat{e}_\mu)U_\mu(x - a\hat{e}_\mu) - (\mu \leftrightarrow \nu)\right]. \tag{12}$$

The portion of the lattice NRQCD action containing the heavy quark-gluon interactions may be written [2]

$$S_Q^{(n)} = a^3\sum_x \psi^\dagger(x)\psi(x)$$

$$-a^3\sum_x \psi^\dagger(x+a\hat{e}_4)\left(1-\frac{a\tilde{H}_0}{2n}\right)^n\left(1-\frac{a\delta H}{2}\right)U_4^\dagger(x)\left(1-\frac{a\delta H}{2}\right)\left(1-\frac{a\tilde{H}_0}{2n}\right)^n\psi(x). \tag{13}$$

This action includes all spin-independent corrections which are suppressed by v^2 relative to the leading terms and all spin-dependent interactions suppressed by factors up to v^4. The heavy quark field $\psi(x)$ is a Pauli spinor corresponding to the two upper components of the original Dirac field. (An analogous action may be written for the heavy antiquark field $\chi(x)$.) The improved kinetic energy is given by

$$\tilde{H}_0 = -\frac{\tilde{\Delta}^{(2)}}{2M} - \frac{a}{4n}\frac{(\Delta^{(2)})^2}{4M^2}, \tag{14}$$

where n is a positive integer. This operator is cleverly constructed to produce a leading error from the lattice approximation of the temporal derivative which can be removed by a redefinition of the quark fields. In this way, the heavy quark propagation remains governed by a Schrödinger equation across a single time slice without affecting energy levels, on-shell scattering amplitudes and other physical quantities. The parameter n was introduced in Ref. [1] to remove instabilities in the evolution of the quark Green's function which occur when the temporal spacing is not small enough to accurately treat the high-momenta modes.

The quark-gluon interactions are as follows:

$$\delta H = \sum_{j=1}^{7} c_j \, V_j, \tag{15}$$

where

$$V_1 = -\frac{(\Delta^{(2)})^2}{8M^3}, \tag{16}$$

$$V_2 = \frac{ig}{8M^2}(\boldsymbol{\Delta}^{(\pm)} \cdot \mathbf{E} - \mathbf{E} \cdot \boldsymbol{\Delta}^{(\pm)}), \tag{17}$$

$$V_3 = -\frac{g}{8M^2}\boldsymbol{\sigma} \cdot (\tilde{\boldsymbol{\Delta}}^{(\pm)} \times \tilde{\mathbf{E}} - \tilde{\mathbf{E}} \times \tilde{\boldsymbol{\Delta}}^{(\pm)}), \tag{18}$$

$$V_4 = -\frac{g}{2M}\boldsymbol{\sigma} \cdot \tilde{\mathbf{B}}, \tag{19}$$

$$V_5 = -\frac{g}{8M^3}\{\boldsymbol{\Delta}^{(2)}, \boldsymbol{\sigma} \cdot \mathbf{B}\}, \tag{20}$$

$$V_6 = -\frac{3g}{64M^4}\{\boldsymbol{\Delta}^{(2)}, \boldsymbol{\sigma} \cdot (\boldsymbol{\Delta}^{(\pm)} \times \mathbf{E} - \mathbf{E} \times \boldsymbol{\Delta}^{(\pm)})\}, \tag{21}$$

$$V_7 = -\frac{ig^2}{8M^3}\boldsymbol{\sigma} \cdot \mathbf{E} \times \mathbf{E}, \tag{22}$$

and where the coefficients c_j are functions of aM and the running coupling α_s in general. At tree level, their values are all unity. Note that the three-vector $\boldsymbol{\Delta}^{(\pm)}$ refers to the spatial components of the covariant four-vector $\Delta_\mu^{(\pm)}$, while $\mathbf{E}$ and $\mathbf{B}$ refer to the components E^k and B^k, respectively.

The four-fermion contact interactions involving a quark and an antiquark $\chi(x)$ are given by:

$$S_{\text{contact}} = -g^4 \frac{a^4}{M^2} \sum_x \Big\{ d_1 \psi^\dagger(x)\chi(x)\chi^\dagger(x)\psi(x) + d_2 \psi^\dagger(x)\boldsymbol{\sigma}\chi(x) \cdot \chi^\dagger(x)\boldsymbol{\sigma}\psi(x)$$
$$+ \sum_{a=1}^{8} \Big(d_3 \psi^\dagger(x) T^a \chi(x) \chi^\dagger(x) T^a \psi(x) + d_4 \psi^\dagger(x) T^a \boldsymbol{\sigma} \chi(x) \cdot \chi^\dagger(x) T^a \boldsymbol{\sigma} \psi(x) \Big) \Big\}. \tag{23}$$

Analogous contact terms between pairs of quarks and pairs of antiquarks also occur but only affect baryons.

The standard Euclidean gluon action is given by

$$\hat{S}_G = a^4 \sum_x \mathcal{L}_G(x), \tag{24}$$

where

$$\mathcal{L}_G(x) = \frac{1}{2a^4 g^2} \sum_{\mu \neq \nu} \mathrm{Tr}[2 - \Omega_{\mu\nu}(x) - \Omega^\dagger_{\mu\nu}(x)] \tag{25}$$

is the usual single-plaquette lattice gauge field Lagrangian density. An improved gluonic action may be written

$$S_G = a^4 \sum_x (\frac{4}{3}\mathcal{L}_G(x) - \frac{1}{3}\mathcal{L}_G^{(2\times 2)}(x)), \tag{26}$$

where $\mathcal{L}_G^{(2\times 2)}$ is comprised of 2×2 plaquette operators and is given by:

$$\mathcal{L}_G^{(2\times 2)}(x) = \frac{1}{32a^4 g^2} \sum_{\mu \neq \nu} \mathrm{Tr}[2 - \Omega^{(2)}_{\mu\nu}(x) - \Omega^{\dagger(2)}_{\mu\nu}(x)], \tag{27}$$

with

$$\Omega^{(2)}_{\mu\nu}(x) = \frac{1}{4} \sum_{\{(\alpha,\beta)\}_{\mu\nu}} U_\alpha(x) U_\alpha(x+a\hat{e}_\alpha) U_\beta(x+2a\hat{e}_\alpha) U_\beta(x+2a\hat{e}_\alpha+a\hat{e}_\beta)$$
$$\times U_{-\alpha}(x+2a\hat{e}_\alpha+2a\hat{e}_\beta) U_{-\alpha}(x+a\hat{e}_\alpha+2a\hat{e}_\beta) U_{-\beta}(x+2a\hat{e}_\beta) U_{-\beta}(x+a\hat{e}_\beta), \tag{28}$$

and $\{(\alpha,\beta)\}_{\mu\nu} = \{(\mu,\nu),(\nu,-\mu),(-\mu,-\nu),(-\nu,\mu)\}$ for $\mu \neq \nu$. Presently, light quarks are neglected.

The lattice NRQCD action is formulated in terms of the link variables $U_\mu(x)$ in order to preserve local gauge invariance, and as the lattice spacing a becomes small, it must tend to the action of the continuum theory. This can be shown at tree level in perturbation theory using the following relationship between the link variables and the gluon field $G_\mu(x)$ of the continuum theory:

$$U_\mu(x) = \exp\left[iagA_\mu(x+\frac{a}{2}\hat{e}_\mu)\right] \sim 1 + iagG_\mu(x), \tag{29}$$

where the lattice gluon field $A_\mu(x) = G_\mu(x) + O(a^2)$. Beyond tree level, however, one observes that large renormalizations are necessary to match the small a limit of the lattice action to the continuum form. These large renormalizations stem mainly from the higher-order powers of agA_μ which occur in the expansion of U_μ. Such terms generate ultraviolet divergences proportional to powers of a^{-1} and so are suppressed only by powers of g^2 and not a.

A simple gauge-invariant procedure for improving the lattice NRQCD action by reducing the magnitudes of the renormalizations needed to reproduce the continuum theory has been suggested: replace all link variables U_μ that appear in the lattice action by U_μ/u_0, where u_0 is a parameter representing the mean value of the link [2]. A gauge-invariant definition of this mean-field parameter may be written in terms of the mean plaquette:

$$u_0 = \langle \frac{1}{3} \mathrm{Tr} U_{\mathrm{plaq}} \rangle^{1/4}. \tag{30}$$

The parameter u_0 may be calculated using perturbation theory or may be measured in a simulation in order to include nonperturbative effects. The mean-field corrections introduced by this procedure are sometimes not small; for example, the cloverleaf magnetic and electric fields may be nearly doubled. Omission of such factors can result in significant underestimates of quantities, such as spin splittings, which depend on $\mathbf{E}$ and $\mathbf{B}$.

In lattice NRQCD simulations, a value for the lattice spacing a must be chosen subject to a few constraints. First, the cutoff $\Lambda \sim \pi/a$ must be larger than the highest physically-relevant mass scale; thus, $\Lambda \gg Mv$ is required. For bottomonium, $v_b^2 \sim 0.1$ and $M_b \sim 5$ GeV so that $a \ll 2.0\ \mathrm{GeV}^{-1}$; for charmonium, $v_c^2 \sim 0.3$ and $M_c \sim 1.7$ GeV yielding $a \ll 3.4\ \mathrm{GeV}^{-1}$. It is also desirable to choose Λ large enough so that $O(g^2(\Lambda))$ corrections to the coupling coefficients c_j and d_j are small. However, NRQCD is a nonrenormalizable effective field theory and its coupling coefficients generally contain powers of Λ/M, causing problems if Λ is made too large. Furthermore, an overly large cutoff defeats the very purpose of NRQCD, which is to remove the scale M from the dynamics. Hence, it is important that Λ does not get much larger than M. Note that the requirement $aL \gg r$, where L is the extent of the lattice in number of sites and r is the root-mean-square radius of the system under study, can be easily satisfied in present-day simulations since $r_\psi \sim 2.4 - 5.0\ \mathrm{GeV}^{-1}$ for the ψ family and $r_\Upsilon \sim 1.0 - 3.6\ \mathrm{GeV}^{-1}$ for bottomonium.

Once a suitable value for a is chosen, the bare quark mass M and the bare lattice coupling g must be fixed by reference to experiment. One very useful quantity for this purpose is the spin-averaged $s-p$ splitting in quarkonium; due to an interplay between the Coulombic and linear forces, this splitting is essentially independent of aM. The masses of the lowest-lying ψ and Υ mesons are also appropriate references. Of course, g and M run with a in such a way that low-energy physical predictions do not depend on the cutoff up to some order in v and a. In practice, it is much more convenient to first choose an appropriate value for g, and then fix a and M by comparison to experiment.

III. THE FEYNMAN RULES

In a lattice gauge theory, the space of gauge transformations is finite so that gauge-fixing is not necessary. However, weak-coupling perturbation theory can only be applied if one fixes the gauge and extends the integration range of $A_\mu^b(x)$ using the familiar Faddeev-Popov technique [5]. Hence, a gauge-fixing term $S_{\rm GF}$ must be added to the NRQCD action. The Faddeev-Popov ghost action can then be determined from $S_{\rm GF}$ [6].

To facilitate the perturbative evaluation of scattering amplitudes, the gauge-invariant path integral measure must be expressed in terms of the lattice gluon field [7]:

$$[\mathcal{D}U] = \exp\left(-S_{\rm ms}\right)\left(\prod_{xb\mu} dA_\mu^b(x)\right), \tag{31}$$

where

$$S_{\rm ms} = -\frac{1}{2}\sum_{x\mu}\mathrm{Tr}\ln\left[\frac{2(1-\cos ag\mathcal{A}_\mu(x+\frac{a}{2}\hat{e}_\mu))}{(ag\mathcal{A}_\mu(x+\frac{a}{2}\hat{e}_\mu))^2}\right] \tag{32}$$

and $\mathcal{A}_\mu^{bc} = if^{bcd}A_\mu^d$. To order g^2,

$$S_{\rm ms} \approx \frac{a^2g^2}{8}\sum_{xb\mu}\left[A_\mu^b(x+\frac{a}{2}\hat{e}_\mu)\right]^2. \tag{33}$$

The Feynman rules are determined by expanding the total action in terms of the coupling g and Fourier transforming into momentum space. The coupling coefficients are written $c_j = 1 + g^2c_j^{(2)} + O(g^4)$. Rewriting the heavy quark-gluon action as

$$S_Q^{(n)} = a^8\sum_{xy}\psi^\dagger(y)G(y;x)\psi(x), \tag{34}$$

then

$$S_Q^{(n)} = \int\frac{d^4k}{(2\pi)^4}\frac{d^4k'}{(2\pi)^4}\,\tilde{\psi}^\dagger(k')\tilde{G}(k';k)\tilde{\psi}(k), \tag{35}$$

where the Fourier transforms are defined on an infinite lattice by:

$$\psi(x) = \int_{|k_\mu|\le\pi/a}\frac{d^4k}{(2\pi)^4}e^{-ik\cdot x}\tilde{\psi}(k), \tag{36}$$

$$\tilde{G}(k';k) = a^8\sum_{xy}e^{ik'\cdot y - ik\cdot x}G(y;x). \tag{37}$$

The perturbative expansion of $\tilde{G}(k';k)$ in terms of the gluon fields takes the general form:

$$\tilde{G}(k';k) = (2\pi)^4\delta^{(4)}(k'-k)\; a^{-1}\xi^{(0)}_{\tilde{G}}(k',k)$$
$$+\sum_{\nu_1 b_1}\int d(k',k;q_1)\;\tilde{A}^{b_1}_{\nu_1}(q_1)\;\xi^{(1)}_{\tilde{G}}(k',k;q_1,\nu_1,b_1)$$
$$+\sum_{\nu_1\nu_2 b_1 b_2}\int d(k',k;q_1,q_2)\;\tilde{A}^{b_1}_{\nu_1}(q_1)\tilde{A}^{b_2}_{\nu_2}(q_2)a\xi^{(2)}_{\tilde{G}}(k',k;q_1,\nu_1,b_1;q_2,\nu_2,b_2)+\;\ldots, \quad (38)$$

where

$$d(k',k;q_1,\ldots,q_r) = \left[\prod_{i=1}^{r}\frac{d^4q_i}{(2\pi)^4}\right](2\pi)^4\delta^{(4)}\left(k'-k+\sum_{i=1}^{r}q_i\right) \quad (39)$$

and $\tilde{A}_\mu(q)$ is the Fourier transform of $A_\mu(x)$ defined by

$$A_\mu(x) = \int\frac{d^4q}{(2\pi)^4}e^{iq\cdot x}\tilde{A}_\mu(q). \quad (40)$$

Thus, the Feynman rules follow easily from the (dimensionless) $\xi^{(i)}_{\tilde{G}}$ functions.

One of the simplest ways to compute the functions $\xi^{(i)}_{\tilde{G}}$ is to first calculate the Fourier transforms of the basic operators which comprise $\tilde{G}(k';k)$ and then combine these Fourier transforms appropriately. The perturbative expansion of the transform of each such operator will take the same general form as that for $\tilde{G}(k';k)$ given above. Of course, this general form also applies to transform products. Let

$$C_{\{\alpha\beta\}}(k';k) = \int\frac{d^4p}{(2\pi)^4}\;A_{\{\alpha\}}(k';p)\;B_{\{\beta\}}(p;k), \quad (41)$$

then the product rule for the ξ functions may be expressed as follows:

$$\xi^{(r)}_{C_{\{\alpha\beta\}}}\left(k',k;\{q_l,\nu_l,b_l\}_{l=1}^{r}\right)$$
$$=\sum_{s=0}^{r}\xi^{(s)}_{A_{\{\alpha\}}}\left(k',k'+\sum_{l=1}^{s}q_l;\{q_i,\nu_i,b_i\}_{i=1}^{s}\right)\xi^{(r-s)}_{B_{\{\beta\}}}\left(k-\sum_{m=s+1}^{r}q_m,k;\{q_j,\nu_j,b_j\}_{j=s+1}^{r}\right). \quad (42)$$

Using this rule and the additivity of the ξ functions, one can quickly build up the $\xi^{(i)}_{\tilde{G}}$ functions. The Fourier transforms of all the necessary basic operators are presented in Appendix A.

The lowest-order heavy quark propagator, shown in Fig. 1(a), is given by:

$$\mathcal{Q}^{ij}_{\alpha\beta}(k) = a\delta^{ij}\delta_{\alpha\beta}Q(k), \quad (43)$$

where i,j are color indices and α,β are spin indices, and

$$Q(k) = \left[1-e^{ik_4a}\left(1+\frac{\kappa_2(\mathbf{k})^2}{M^3a^3}\right)^2\left(1-\frac{\kappa_2(\mathbf{k})}{nMa}-\frac{\kappa_4(\mathbf{k})}{3nMa}+\frac{\kappa_2(\mathbf{k})^2}{2n^2M^2a^2}\right)^{2n}\right]^{-1} \quad (44)$$

with $\kappa_n(\mathbf{k}) = \sum_{j=1}^{3} \sin^n(k_j a/2)$.

In the Feynman gauge, the lowest-order gluon propagator, shown in Fig. 1(b), is given by:

$$\mathcal{D}^{bc}_{\eta\nu}(k;\lambda) = a^2 \delta^{bc} \delta_{\eta\nu} D_\nu(k;\lambda), \tag{45}$$

where

$$D_\nu(k;\lambda) = \Big[\frac{16}{3}\Big(\sum_{\alpha=1}^{4} \sin^2\Big(\frac{k_\alpha a}{2}\Big)\Big) - \frac{1}{3}\cos^2\Big(\frac{k_\nu a}{2}\Big)\Big(\sum_{\alpha=1}^{4} \sin^2(k_\alpha a)\Big) + a^2\lambda^2\Big]^{-1}. \tag{46}$$

A small gluon mass λ has been introduced to provide an infrared cutoff. If the simple gluon action in Eq. (24) is used, the lowest-order gluon propagator is then

$$\hat{\mathcal{D}}^{bc}_{\eta\nu}(k;\lambda) = a^2 \delta^{bc} \delta_{\eta\nu} \hat{D}(k;\lambda), \tag{47}$$

where

$$\hat{D}(k;\lambda) = \Big[4\Big(\sum_{\alpha=1}^{4} \sin^2\Big(\frac{k_\alpha a}{2}\Big)\Big) + a^2\lambda^2\Big]^{-1}. \tag{48}$$

The lowest-order vertex factors corresponding to interactions involving a heavy quark line and one to three gluons, shown in Fig. 1(c), may be written:

$$\mathcal{V}_1(k',\alpha,i;k,\beta,j;q_1,\nu_1,b_1) = -g\ (2\pi)^4 \delta^{(4)}\Big(k'-k+q_1\Big) \sum_{\mu=1}^{4} \sigma^\mu_{\alpha\beta}\ T^{b_1}_{ij}\ \zeta^{(1)}_{\tilde{G}_0\mu}(k',k;q_1,\nu_1), \tag{49}$$

$$\mathcal{V}_2(k',\alpha,i;k,\beta,j;q_1,\nu_1,b_1;q_2,\nu_2,b_2) = -ag^2\ (2\pi)^4 \delta^{(4)}\Big(k'-k+q_1+q_2\Big) \sum_{\mu=1}^{4} \sigma^\mu_{\alpha\beta} \sum_{\tau\in\mathcal{P}_2} \Big(T^{b_{\tau_1}} T^{b_{\tau_2}}\Big)_{ij} \zeta^{(2)}_{\tilde{G}_0\mu}(k',k;q_{\tau_1},\nu_{\tau_1};q_{\tau_2},\nu_{\tau_2}), \tag{50}$$

$$\mathcal{V}_3(k',\alpha,i;k,\beta,j;q_1,\nu_1,b_1;q_2,\nu_2,b_2;q_3,\nu_3,b_3) = -a^2g^3\ (2\pi)^4 \delta^{(4)}\Big(k'-k+q_1+q_2+q_3\Big) \sum_{\mu=1}^{4} \sigma^\mu_{\alpha\beta} \sum_{\tau\in\mathcal{P}_3} \Big[\Big(T^{b_{\tau_1}} T^{b_{\tau_2}} T^{b_{\tau_3}}\Big)_{ij} \zeta^{(3a)}_{\tilde{G}_0\mu}(k',k;q_{\tau_1},\nu_{\tau_1};q_{\tau_2},\nu_{\tau_2};q_{\tau_3},\nu_{\tau_3}) + \delta_{ij}\mathrm{Tr}\Big(T^{b_{\tau_1}} T^{b_{\tau_2}} T^{b_{\tau_3}}\Big) \zeta^{(3b)}_{\tilde{G}_0\mu}(k',k;q_{\tau_1},\nu_{\tau_1};q_{\tau_2},\nu_{\tau_2};q_{\tau_3},\nu_{\tau_3})\Big], \tag{51}$$

where $\mathcal{P}_r$ is the group of permutations of r elements, σ^k are the standard Pauli spin matrices for $k = 1,2,3$ and σ^4 is a 2×2 identity matrix in spin space. The $\zeta_{\tilde{G}_0}$ functions are obtained from the $\xi_{\tilde{G}}$ functions by neglecting the $O(g^2)$ corrections to the c_j coupling coefficients. These corrections show up in higher-order counterterms.

Link variable renormalization in perturbation theory leads to the addition of the following order g^2 counterterm, shown in Fig. 1(d):

$$\mathcal{V}_{u_0}(k',\alpha,i;k,\beta,j) = -u_0^{(2)}\,\frac{g^2}{a}(2\pi)^4\delta^{(4)}\Big(k'-k\Big)\delta_{\alpha\beta}\delta_{ij}e^{ik_4 a}$$
$$\left(1-\frac{\kappa_2(\mathbf{k})}{nMa}-\frac{\kappa_4(\mathbf{k})}{3nMa}+\frac{\kappa_2(\mathbf{k})^2}{2n^2M^2a^2}\right)^{2n-1}\left(1+\frac{\kappa_2(\mathbf{k})^2}{M^3a^3}\right)$$
$$\left\{\left(1-\frac{6\kappa_2(\mathbf{k})}{M^3a^3}+\frac{5\kappa_2(\mathbf{k})^2}{M^3a^3}\right)\left(1-\frac{\kappa_2(\mathbf{k})}{nMa}-\frac{\kappa_4(\mathbf{k})}{3nMa}+\frac{\kappa_2(\mathbf{k})^2}{2n^2M^2a^2}\right)\right.$$
$$\left.+\left(1+\frac{\kappa_2(\mathbf{k})^2}{M^3a^3}\right)\left(\frac{7}{2Ma}-\frac{4\kappa_2(\mathbf{k})}{3Ma}-\frac{4\kappa_4(\mathbf{k})}{3Ma}-\frac{3\kappa_2(\mathbf{k})}{nM^2a^2}+\frac{2\kappa_2(\mathbf{k})^2}{nM^2a^2}\right)\right\}, \qquad (52)$$

writing $u_0 = 1 + u_0^{(2)}g^2 + O(g^4)$.

The goal here is to determine the numerical values of the coupling coefficients c_j and d_j and various renormalization factors for given values of the input parameters needed in lattice simulations, namely, the bare lattice coupling g and the bare heavy quark mass aM. Since these couplings and renormalization factors essentially absorb the relativistic effects arising from highly-ultraviolet processes, one expects that they may be calculated to a good approximation using weak-coupling perturbation theory. Using the above Feynman rules, the development of perturbative expansions for these quantities in terms of g is straightforward. However, there is no compelling reason to use the bare lattice coupling for the expansion parameter. In fact, recent work [8] suggests that g is a very poor choice of expansion parameter and that much better perturbation series result if one re-expresses the series in terms of a renormalized coupling g_r defined in terms of some physical quantity and which runs with the relevant length scale. This is standard practice in continuum perturbation theory. Of course, if calculations could be carried out to all orders, then the choice of expansion parameter would be immaterial.

To define a renormalized expansion parameter, a definition of the running coupling $g_r(\mu)$ and a procedure for determining the relevant mass scale μ must be given. A renormalization scheme [8] which defines the coupling such that the heavy quark potential has no g_r^4 or higher order corrections is particularly attractive. This scheme is physically motivated and produces $O(g_r^2)$ perturbative results in good agreement with simulation results for several different quantities. By absorbing the higher-order contributions to the heavy quark potential into g_r^2, it is hoped that higher-order contributions in other quantities will be small. The renormalized coupling $g_r(\mu)$ is then given by the usual two-loop formula with $\Lambda = 46.08\Lambda_{lat}$. The scale μ is determined by averaging $\ln q^2$ over the one-loop process of interest, where q is the loop momentum. Since the heavy quark parameters calculated here are ultraviolet divergent quantities, one expects $\mu \approx \pi/a$. Here, $\bar{g}_r$ shall be used to denote the value $g_r(\mu)$ of the renormalized coupling at the appropriate scale. For example, at $\beta = 5.7$, $g_r^2(\pi/a) \approx 1.9$ and at $\beta = 6.0$, $g_r^2(\pi/a) \approx 1.7$. Alternatively, $\bar{g}_r$ could simply be

added to the list of parameters which must be fixed in any simulation by reference to experiment.

IV. THE HEAVY QUARK SELF-ENERGY

The heavy quark self-energy $\Sigma(p)$ may be defined by writing the inverse quark propagator $\mathcal{G}^{-1}(p)$ in the form

$$a\mathcal{G}^{-1}(p)^{ij}_{\alpha\beta} = Q^{-1}(p)\delta^{ij}\delta_{\alpha\beta} - a\Sigma^{ij}_{\alpha\beta}(p), \tag{53}$$

where i, j are color indices and α, β are spin indices. At order g^2 and v^4 and neglecting link variable renormalization for the moment, this self-energy is given by:

$$\Sigma^{ij}_{\alpha\beta}(p) = \lim_{\lambda\to 0} g^2\delta^{ij}\delta_{\alpha\beta}(\Sigma^{(A)}(p;\lambda) + \Sigma^{(B)}(p;\lambda)), \tag{54}$$

where

$$a\Sigma^{(A)}(p;\lambda) = \frac{4}{3}a^4 \sum_{\mu,\nu=1}^{4} \int \frac{d^4k}{(2\pi)^4} Q(p-k)D_\nu(k;\lambda)\ \varepsilon_\mu[\zeta^{(1)}_{\tilde{G}_0\mu}(p-k,p;k,\nu)]^2, \tag{55}$$

corresponding to the diagram in Fig. 2(a), and

$$a\Sigma^{(B)}(p;\lambda) = -\frac{4}{3}a^4 \sum_{\nu=1}^{4} \int \frac{d^4k}{(2\pi)^4} D_\nu(k;\lambda)\zeta^{(2)}_{\tilde{G}_0 4}(p,p;k,\nu;-k,\nu), \tag{56}$$

corresponding to the tadpole diagram in Fig. 2(b). Note that $\varepsilon_\mu = (-1,-1,-1,1)$. The following properties of the ζ functions are used to obtain the above results:

$$\zeta^{(1)}_{\tilde{G}_0\mu}(k',k;k-k',\nu) = \varepsilon_\mu\ \zeta^{(1)}_{\tilde{G}_0\mu}(k,k';k'-k,\nu), \tag{57}$$

$$\zeta^{(2)}_{\tilde{G}_0 j}(p,p;k,\nu;-k,\nu) = 0, \qquad (j=1,2,3). \tag{58}$$

The self-energy is invariant under spatial reflections $p_j \to -p_j$, for $j = 1,2,3$, and transforms into its complex conjugate under $p_4 \to -p_4^*$.

In order to investigate $\Sigma^{(A)}(p;\lambda)$ and $\Sigma^{(B)}(p;\lambda)$ in the neighborhood of $p = 0$, the integrals in Eqs. (55) and (56) must first be evaluated. The usual initial step in the determination of such integrals is to use the change of variables $z = \exp(\pm ik_4 a)$ to transform the integral over k_4 into a contour integral along the $|z| = 1$ unit circle. Unfortunately, the complicated pole structure of the vertex factors near $z = 0$ makes difficult the evaluation of this contour integral by the residue theory. Due to this fact, the simplest procedure, approximating the four-dimensional integral by an appropriate summation as described below, is preferred.

Because the integrand in Eq. (56) is a periodic analytic function of the real variables k_μ with period 2π when $\lambda > 0$, $\Sigma^{(B)}(p;\lambda)$ is numerically well approximated by the discrete sum

$$a\Sigma^{(B)}(p;\lambda) \approx -\frac{4}{3}\frac{1}{N^4}\sum_k \sum_{\nu=1}^{4} D_\nu(k;\lambda)\zeta^{(2)}_{\tilde{G}_0 4}(p,p;k,\nu;-k,\nu). \tag{59}$$

In this sum, $ak_\mu = 2\pi n_\mu/N$ where the n_μ take all integer values satisfying $-N/2 < n_\mu \leq N/2$ for integral N. The error resulting from this approximation diminishes exponentially fast as $N \to \infty$. However, the rate of decay of this error is directly proportional to the mass gap $a\lambda$, creating difficulties when $a\lambda$ is small. Fortunately, the decay rate of this error can be dramatically increased by making the following change of variables [9]: $k_\mu \to k_\mu - \alpha\sin(k_\mu)$ with $0 \leq \alpha < 1$. This transformation maintains periodicity and effectively increases the mass gap so that the approximation

$$a\Sigma^{(B)}(p;\lambda) \approx -\frac{4}{3}\frac{1}{N^4}\sum_k \sum_{\nu=1}^{4} \varrho(k) D_\nu(s(k);\lambda)\zeta^{(2)}_{\tilde{G}_0 4}(p,p;s(k),\nu;-s(k),\nu), \tag{60}$$

where $s_\mu(k) = k_\mu - \alpha\sin(k_\mu)$ and $\varrho(k) = \prod_{\mu=1}^{4}[1-\alpha\cos(k_\mu)]$, converges much more quickly as N is increased. The parameter α should be chosen so as to maximize the effective mass gap: $\alpha = \mathrm{sech}(u)$, where u satisfies $a\lambda \approx u - \tanh(u)$.

The above procedure is sufficient for evaluating $\Sigma^{(B)}(p;\lambda)$ as long as the gluon mass $a\lambda$ is not set too small. However, the pole in the quark propagator is problematical when evaluating $\Sigma^{(A)}(p;\lambda)$ near $p = 0$. To circumvent this, the contour for the ak_4 integral, which runs along the real axis from $-\pi$ to π except near the pole, can be continuously deformed into a contour consisting of three line segments passing through the points $-\pi \to -\pi - ia\lambda/2 \to \pi - ia\lambda/2 \to \pi$. This contour is chosen for the following two reasons: for $p \sim 0$, the distance of closest approach to any pole is a maximum; and the contributions from the segments of the contour running parallel to the imaginary axis cancel due to the periodicity of the integrand. $\Sigma^{(A)}(p \sim 0;\lambda)$ can then be accurately obtained using the following approximation:

$$\begin{aligned} a\Sigma^{(A)}(p\sim 0;\lambda) \approx \frac{4}{3}\frac{1}{N^4}\sum_k \sum_{\mu,\nu=1}^{4} \varrho(k) Q(p-r(k)) \\ \times D_\nu(r(k);\lambda)\varepsilon_\mu\left[\zeta^{(1)}_{\tilde{G}_0\mu}(p-r(k),p;r(k),\nu)\right]^2, \end{aligned} \tag{61}$$

where $r_\mu(k) = k_\mu - \alpha\sin(k_\mu) - ia\lambda\delta_{4,\mu}/2$ and $ak_\mu = 2\pi n_\mu/N$ with the n_μ taking all integer values satisfying $-N/2 < n_\mu \leq N/2$. Also, $\alpha = \mathrm{sech}(y)$ and $a\lambda/2 \approx y - \tanh(y)$. In practice, the approximations in Eqs. (60) and (61) are applied using increasing values of N until sufficient convergence is observed; typically, $N = 20$ is adequate. Note that for values of p satisfying $p_x = p_y = p_z$, the number of terms which must be independently evaluated in these sums may be dramatically reduced by exploiting the invariance of the summands under interchange of any two spatial components of k.

The evaluation of $\Sigma^{(A)}(p \sim 0;\lambda)$ and $\Sigma^{(B)}(p \sim 0;\lambda)$ using Eqs. (61) and (60) is feasible only if the gluon mass λ is not set too small. However, the limits of these

functions as $\lambda \to 0$ are actually required, necessitating the use of an extrapolation procedure. The expected behavior of these quantities as λ tends to zero may be expressed as an asymptotic expansion of the form

$$\Sigma(p;\lambda) \underset{\lambda\to 0+}{\sim} \sum_{m=0}^{\infty} \left(b_m^{(0)} + b_m^{(1)} \ln a^2\lambda^2\right) (a\lambda)^m, \tag{62}$$

where the coefficient $b_0^{(1)}$ is known from the continuum theory since the infrared divergence is insensitive to the ultraviolet regulator. If one neglects the $b_m^{(1)}$ terms for $m > 0$, then polynomial extrapolation using Neville's algorithm may be applied to $f_0(p;\lambda) = \Sigma(p;\lambda) - b_0^{(1)} \ln a^2\lambda^2$. The extrapolation can be improved by applying Neville's algorithm to the function $f_1(p;\lambda) = f_0(p;\lambda) - a\lambda\partial_{(a\lambda)}\Sigma(p;\lambda) + 2b_0^{(1)}$ which has no $a\lambda \ln a^2\lambda^2$ term. Polynomial extrapolation of $f_2(p;\lambda) = f_1(p;\lambda) + (a^2\lambda^2/2)\partial^2_{(a\lambda)}\Sigma(p;\lambda) + b_0^{(1)}$, which does not suffer from $a^2\lambda^2 \ln a^2\lambda^2$ and $a\lambda \ln a^2\lambda^2$ effects, is another method. Since the gluon mass appears only in the gluon propagator, the derivatives of $\Sigma(p;\lambda)$ with respect to $a\lambda$ can be exactly and efficiently taken. In practice, polynomial extrapolation of all three functions $f_0(p;\lambda)$, $f_1(p;\lambda)$, and $f_2(p;\lambda)$ is done using between six and twelve values of the gluon mass lying in the range $0.15 \le a\lambda \le 0.8$, and agreement among the results is verified. In calculating $\Sigma^{(B)}(p;\lambda \to 0)$, one finds that only even powers of $a\lambda$ occur in its asymptotic expansion. In this case, the accuracy of the extrapolation can be increased by explicitly excluding the odd powers in the extrapolating polynomial. Neville's algorithm is then applied to the functions $f_0(p;\lambda)$, $\tilde{f}_1(p;\lambda) = f_0(p;\lambda) - a^2\lambda^2\partial_{(a^2\lambda^2)}\Sigma(p;\lambda) + b_0^{(1)}$ and $\tilde{f}_2(p;\lambda) = \tilde{f}_1(p;\lambda) + (a^4\lambda^4/2)\partial^2_{(a^2\lambda^2)}\Sigma(p;\lambda) + b_0^{(1)}/2$. Uncertainties in the extrapolated values are estimated by examining the spread of values in the Neville table and by comparing the results obtained using different sets of gluon mass values and using the different functions described above.

The small v expansion of the zeroth-order heavy quark inverse propagator, keeping only those terms which are suppressed by no more than v^2 relative to the leading terms, is given by:

$$Q^{-1}(p) \approx -ip_4 a + \frac{\mathbf{p}^2 a^2}{2Ma} + \frac{p_4^2 a^2}{2} + \frac{ip_4 \mathbf{p}^2 a^3}{2Ma} - \frac{(\mathbf{p}^2)^2 a^4}{8M^3 a^3} - \frac{(\mathbf{p}^2)^2 a^4}{8M^2 a^2} + \ldots, \tag{63}$$

recalling that p_4 is of order v^2. The on-mass-shell quark then satisfies the following dispersion relation:

$$\omega_0(\mathbf{p}) \approx i\Big(\frac{\mathbf{p}^2}{2M} - \frac{(\mathbf{p}^2)^2}{8M^3} + \ldots\Big), \tag{64}$$

where $\omega_0(\mathbf{p})$ denotes the value of the fourth component of the contravariant quark four-momentum p^μ at the pole of the zeroth-order propagator. This dispersion relation agrees exactly with the continuum form from full QCD to this order in v.

In the $\overline{MS}$ renormalization scheme, the inverse propagator to order g^2 for full QCD in continuum Minkowski space has the form

$$(1 - C_{cont}g^2)\left(\not{p} - M(1 + \delta_{cont}g^2)\right) \tag{65}$$

where

$$C_{cont} = \frac{1}{12\pi^2}\left(-4 + \ln(M^2/\mu^2) + 2\ln(M^2/\lambda^2)\right), \tag{66}$$

$$\delta_{cont} = \frac{1}{12\pi^2}\left(4 + 3\ln(\mu^2/M^2)\right). \tag{67}$$

Note that μ is the mass scale introduced by dimensional regularization and λ is the gluon mass regulating the infrared divergence. Thus, the sole effect of the order g^2 corrections is to renormalize the quark field and mass. If lattice NRQCD is to reproduce the low-energy physical predictions of full QCD, then the order g^2 corrections to the heavy quark propagator in lattice NRQCD must also do no more than renormalize the heavy quark field and mass to the appropriate order in v.

Explicit calculation shows that the heavy quark self-energy in lattice NRQCD has a small v representation of the following form:

$$a\Sigma(p) \approx g^2\Big\{\Omega_0 - ip_4a\Omega_1 + \frac{\mathbf{p}^2a^2}{2Ma}\Omega_2 + \ldots\Big\}, \tag{68}$$

retaining only radiative corrections to the lowest-order terms in v as specified by the power counting rules of Ref. [2]. The on-mass-shell quark now satisfies a dispersion relation given by

$$\omega_0(\mathbf{p}) \approx i\Big(-g^2\Omega_0/a + \frac{\mathbf{p}^2}{2M}\left(1 + g^2\Omega_1 - g^2\Omega_2\right) - \frac{(\mathbf{p}^2)^2}{8M^3} + \ldots\Big). \tag{69}$$

Defining $M_r = Z_mM$, where $Z_m = 1 - g^2\Omega_1 + g^2\Omega_2$ is the mass renormalization factor, and $\bar{p}_4 = p_4 - ig^2\Omega_0/a$, the inverse propagator for small v may be written:

$$a\mathcal{G}^{-1}(p) \approx Z_\psi\left(-i\bar{p}_4a + \frac{\mathbf{p}^2a^2}{2M_ra} + \frac{\bar{p}_4^2a^2}{2} + \frac{i\bar{p}_4\mathbf{p}^2a^3}{2M_ra} - \frac{(\mathbf{p}^2)^2a^4}{8M_r^3a^3} - \frac{(\mathbf{p}^2)^2a^4}{8M_r^2a^2} + \ldots\right), \tag{70}$$

where $Z_\psi = 1 - g^2(\Omega_0 + \Omega_1)$ is the wavefunction renormalization parameter. Thus, the addition of a counterterm which shifts the energy by an overall amount $\bar{g}_r^2\Omega_0/a$ is needed in order to match the low-energy physical predictions of lattice NRQCD with those of QCD. Alternatively, one could simply shift the energies obtained in simulations using the action in Eq. 13 by an amount $\bar{g}_r^2\Omega_0/a$ for each heavy quark.

A more convenient set of renormalization parameters may be obtained by defining $Z_\psi = 1 - g^2C$, $Z_m = 1 + g^2B$, and $\bar{p}_4 = p_4 + ig^2A/a$. The parameters A, B, and C can then be calculated using $A = -\Omega_0$, $B = \Omega_2 - \Omega_1$, and $C = \Omega_0 + \Omega_1$, where $\Omega_0 = a\Sigma(0)/g^2$, $\Omega_1 = ia\partial_{p_4a}\Sigma(0)/g^2$, and $\Omega_2 = 2Ma^2\partial_{\mathbf{p}^2a^2}\Sigma(0)/g^2$. Due to the complexity of the NRQCD vertex factors, the derivatives in these expressions must

be taken numerically. Four- and five-point formulas are applied in the differentiation; only points which satisfy $p_x = p_y = p_z$ are used since the self-energy can be computed much more quickly at such points.

Results for the energy shift parameter A and the mass renormalization parameter B are presented in Tables I and II, respectively. Both A and B are gauge invariant and infrared finite. The wavefunction renormalization parameter C has an infrared divergence of the form $-(\ln a^2\lambda^2)/6\pi^2$ as the gluon mass is taken to zero. This divergence is cancelled in physical quantities by an infrared divergence occurring in the quark-gluon vertex correction. Values for the infrared-finite portion of C are given in Table III. In these tables, the contributions from the quark-gluon loop and tadpole diagrams are given separately. Results using the simple and the improved gluonic actions are presented. Values for the stability parameter n are chosen such that the pole in the quark propagator $Q(p)$ falls on the same side of the real axis in the complex p_4 plane for all allowed values of $\mathbf{p}$ and tends to move farther away from this real axis as $|\mathbf{p}|$ increases to its allowed maximum. For $aM \geq 2$, n is set to unity; for $1 \leq aM < 2$, $n = 2$ is used. These values of n ensure the stability of the evolution equation for the quark Green's function.

Contributions from the quark-gluon loop graph to the energy shift parameter A are small and decrease in magnitude as aM decreases. At large aM, there is little difference between the shifts obtained using the simple and improved gluonic actions. The tadpole contributions are large and contain power-law divergences which grow in magnitude as aM is decreased. Since high-momentum modes are more strongly damped in the improved gluon propagator, the ultraviolet-divergent tadpole terms are appreciably smaller in the case of the improved gluon action. These total downward shifts in the energy are nearly the same as those obtained in Ref. [3] which used a much simpler heavy quark action. Calculations of A using $c_j = 0$ for $j = 3, 4, 5, 6, 7$ reveal that contributions to this parameter from the spin-dependent interactions are small.

Contributions to the mass renormalization parameter B from the quark-gluon loop diagram are very small and do not vary proportionately with aM. For all values of aM, there is little difference between the results obtained using the simple and the improved gluon actions. The tadpole contributions are again large, growing in magnitude as aM is decreased. The tadpole terms in the case of the improved action are slightly smaller and contributions to this parameter from the spin-dependent interactions are small. The total values for B obtained here are appreciably larger than the order g^2 corrections to the mass renormalization calculated in Ref. [3] (see Ref. [10]).

The tadpole diagrams do not contribute to the heavy quark wavefunction renormalization parameter C. The values for the infrared-finite portion of C are very small and become increasingly negative as aM is decreased. There is little difference between the results obtained using the simple and the improved gluonic actions. The magnitudes of the wavefunction renormalization corrections are much smaller than

those obtained in Ref. [3] (see Ref. [10]).

The contributions to the energy shift and mass renormalization parameters from the link variable renormalization counterterm are given by:

$$\delta A = u_0^{(2)} \left(1 + \frac{7}{2Ma}\right), \tag{71}$$

$$\delta B = u_0^{(2)} \left(\frac{2}{3} - \frac{1}{4nMa} + \frac{3}{M^2a^2}\right). \tag{72}$$

No change in the wavefunction renormalization occurs. As previously stated, the purpose of link variable renormalization is to enhance the similarities between lattice and continuum gauge-field operators, especially those depending on the cloverleaf electric and magnetic fields. Consequently, the counterterms introduced by this renormalization offset the large tadpole contributions which commonly afflict lattice perturbation theory, offering a means of improving its convergence. As shown in Table IV, the order g^2 corrections to the heavy quark renormalization parameters are small once the mean-field corrections are taken into account. In this table, the value $u_0^{(2)} = -0.083$ obtained by evaluating Eq. 30 in perturbation theory for the simple gluonic action is used. For $\bar{g}_r^2 \sim 2$ and $a \sim 1\text{GeV}^{-1}$, the b quark receives approximately a 1% lowest-order correction to its mass and the c quark receives about a 7% mass correction.

V. CONCLUSION

Lattice NRQCD is an effective field theory which promises to make possible high-precision numerical studies of heavy quark systems. It is essentially a low-energy expansion of QCD in terms of the mean velocity of the heavy quarks in a typical heavy-quark hadron. To fully define lattice NRQCD, the coupling strengths of its interactions must be specified. These are determined by requiring that lattice NRQCD reproduces the low-energy physical results of continuum QCD. Since the role of these couplings is to absorb the relativistic effects arising from highly-ultraviolet QCD processes, one expects that they may be computed to a good approximation using perturbation theory, provided the quark mass M is large enough.

The heavy quark self-energy in nonrelativistic lattice QCD was calculated to $O(\alpha_s)$ in perturbation theory. An action which includes all spin-independent relativistic corrections to order v^2 and all spin-dependent corrections to order v^4 was used. The standard Wilson action and an improved multi-plaquette action were used for the gluons. Results for the mass and wavefunction renormalization and an overall energy shift were obtained. Contributions from the quark-gluon loop graph were found to be very small; however, the tadpole contributions were large. The values of these parameters will be needed in future numerical simulations of quarkonium. The effective couplings will also be needed; calculation of these quantities is in progress.

A tadpole improvement scheme in which all link variables are rescaled by a mean-field factor u_0 was also applied in perturbation theory. The main purpose of this link

variable renormalization was to enhance the similarities between lattice and continuum gauge-field operators, especially those depending on the cloverleaf electric and magnetic fields. An important consequence of this scheme was a significant offsetting of the large tadpole contributions to the heavy quark renormalization parameters. Using a perturbative approximation to the mean plaquette for u_0, the tadpole-improved heavy quark renormalization parameters were shown to be small. This scheme offers a means of improving the convergence properties of lattice perturbation theory.

ACKNOWLEDGMENTS

I would like to thank G. Peter Lepage for many useful conversations. This work was supported by the Natural Sciences and Engineering Research Council of Canada and by the Department of Energy, Contract No. DE-AC03-76SF00515.

APPENDIX A

The momentum-space representations of various components of the lattice NRQCD action are presented in this Appendix. Below, ζ functions are introduced and are defined by

$$\xi_A^{(r)}(k',k;q_1,\nu_1,b_1;\ldots;q_r,\nu_r,b_r) = g^r \zeta_A^{(r)}(k',k;q_1,\nu_1;\ldots;q_r,\nu_r)\; T^{b_1}\cdots T^{b_r}. \quad \text{(A1)}$$

Also note that $\bar{\delta}_{\mu\nu}$ is an "anti-Kronecker delta function" and is trivial when $\mu = \nu$ and unity otherwise.

In momentum space, the link variable becomes

$$\begin{aligned} U_\mu(k';k) &= a^4 \sum_x e^{i(k'-k)\cdot x} e^{-ik_\mu a} \exp\left[iagA_\mu(x+\frac{a}{2}\hat{e}_\mu)\right] \\ &= (2\pi)^4\delta^{(4)}(k'-k)e^{-ia(k'_\mu+k_\mu)/2} + iag\int d(k',k;q)e^{-ia(k'_\mu+k_\mu)/2}\tilde{A}_\mu(q) \\ &-\frac{a^2g^2}{2}\int d(k',k;q_1,q_2)e^{-ia(k'_\mu+k_\mu)/2}\tilde{A}_\mu(q_1)\tilde{A}_\mu(q_2) \\ &-\frac{ia^3g^3}{6}\int d(k',k;q_1,q_2,q_3)e^{-ia(k'_\mu+k_\mu)/2}\tilde{A}_\mu(q_1)\tilde{A}_\mu(q_2)\tilde{A}_\mu(q_3)+\cdots. \end{aligned} \quad \text{(A2)}$$

The momentum-space representation of $\Delta_\mu^{(\pm)}$ may be written:

$$\begin{aligned} \zeta^{(0)}_{a\Delta_\mu^{(\pm)}}(k',k) &= -i\sin[\frac{a}{2}(k'+k)_\mu], \\ \zeta^{(1)}_{a\Delta_\mu^{(\pm)}}(k',k;q_1,\nu_1) &= ia\cos[\frac{a}{2}(k'+k)_\mu]\;\delta_{\mu,\nu_1}, \\ \zeta^{(2)}_{a\Delta_\mu^{(\pm)}}(k',k;q_1,\nu_1;q_2,\nu_2) &= i\frac{a^2}{2}\sin[\frac{a}{2}(k'+k)_\mu]\;\delta_{\mu,\nu_1}\delta_{\mu,\nu_2}, \\ \zeta^{(3)}_{a\Delta_\mu^{(\pm)}}(k',k;q_1,\nu_1;q_2,\nu_2;q_3,\nu_3) &= -i\frac{a^3}{6}\cos[\frac{a}{2}(k'+k)_\mu]\;\delta_{\mu,\nu_1}\delta_{\mu,\nu_2}\delta_{\mu,\nu_3}. \end{aligned} \quad \text{(A3)}$$

The improved symmetric derivative has the following momentum-space representation:

$$\zeta^{(0)}_{a\tilde{\Delta}^{(\pm)}_{\mu}}(k',k) = i\left(-\frac{4}{3}\sin[\frac{a}{2}(k'+k)_\mu] + \frac{1}{6}\sin[a(k'+k)_\mu]\right), \tag{A4}$$

$$\zeta^{(1)}_{a\tilde{\Delta}^{(\pm)}_{\mu}}(k',k;q_1,\nu_1) = i\frac{a}{3}\delta_{\mu,\nu_1}\left(4\cos[\frac{a}{2}(k'+k)_\mu] - \cos[a(k'+k)_\mu]\cos(\frac{a}{2}q_{1\mu})\right),$$

$$\zeta^{(2)}_{a\tilde{\Delta}^{(\pm)}_{\mu}}(k',k;q_1,\nu_1;q_2,\nu_2) = ia^2\delta_{\mu,\nu_1}\delta_{\mu,\nu_2}\left(\frac{2}{3}\sin[\frac{a}{2}(k'+k)_\mu]\right.$$
$$\left. -\frac{1}{3}\sin[a(k'+k)_\mu]\cos(\frac{a}{2}q_{1\mu})\cos(\frac{a}{2}q_{2\mu}) - \frac{1}{6}\cos[a(k'+k)_\mu]\sin[\frac{a}{2}(q_1-q_2)_\mu]\right),$$

$$\zeta^{(3)}_{a\tilde{\Delta}^{(\pm)}_{\mu}}(k',k;q_1,\nu_1;q_2,\nu_2;q_3,\nu_3) = ia^3\delta_{\mu,\nu_1}\delta_{\mu,\nu_2}\delta_{\mu,\nu_3}\left(-\frac{2}{9}\cos[\frac{a}{2}(k'+k)_\mu]\right.$$
$$\left. +\frac{1}{18}\cos[a(k'+k)_\mu]\cos[\frac{a}{2}(k'-k)_\mu] + \frac{1}{6}\cos[a(k'+k+\frac{1}{2}q_1-\frac{1}{2}q_3)_\mu]\cos(\frac{a}{2}q_{2\mu})\right).$$

The Fourier transform of the lattice Laplacian may be written:

$$\zeta^{(0)}_{a^2\Delta^{(2)}}(k',k) = -4\sum_{j=1}^{3}\sin^2[\frac{a}{4}(k'+k)_j],$$
$$\zeta^{(1)}_{a^2\Delta^{(2)}}(k',k;q_1,\nu_1) = 2a\sin[\frac{a}{2}(k'+k)_{\nu_1}]\ \bar{\delta}_{4,\nu_1},$$
$$\zeta^{(2)}_{a^2\Delta^{(2)}}(k',k;q_1,\nu_1;q_2,\nu_2) = -a^2\cos[\frac{a}{2}(k'+k)_{\nu_1}]\ \delta_{\nu_1,\nu_2}\bar{\delta}_{4,\nu_1}, \tag{A5}$$
$$\zeta^{(3)}_{a^2\Delta^{(2)}}(k',k;q_1,\nu_1;q_2,\nu_2;q_3,\nu_3) = -\frac{a^3}{3}\sin[\frac{a}{2}(k'+k)_{\nu_1}]\ \delta_{\nu_1,\nu_2}\delta_{\nu_2,\nu_3}\bar{\delta}_{4,\nu_1}.$$

Similarly for the improved Laplacian:

$$\zeta^{(0)}_{a^2\tilde{\Delta}^{(2)}}(k',k) = -4\sum_{j=1}^{3}\left(\sin^2[\frac{a}{4}(k'+k)_j] + \frac{1}{3}\sin^4[\frac{a}{4}(k'+k)_j]\right), \tag{A6}$$

$$\zeta^{(1)}_{a^2\tilde{\Delta}^{(2)}}(k',k;q_1,\nu_1) = \frac{a}{3}\bar{\delta}_{4,\nu_1}\left(8\sin[\frac{a}{2}(k'+k)_{\nu_1}] - \sin[a(k'+k)_{\nu_1}]\cos(\frac{a}{2}q_{1\nu_1})\right),$$

$$\zeta^{(2)}_{a^2\tilde{\Delta}^{(2)}}(k',k;q_1,\nu_1;q_2,\nu_2) = a^2\delta_{\nu_1,\nu_2}\bar{\delta}_{4,\nu_1}\left(-\frac{4}{3}\cos[\frac{a}{2}(k'+k)_{\nu_1}]\right.$$
$$\left. +\frac{1}{3}\cos[a(k'+k)_{\nu_1}]\cos(\frac{a}{2}q_{1\nu_1})\cos(\frac{a}{2}q_{2\nu_1}) - \frac{1}{6}\sin[a(k'+k)_{\nu_1}]\sin[\frac{a}{2}(q_1-q_2)_{\nu_1}]\right),$$

$$\zeta^{(3)}_{a^2\tilde{\Delta}^{(2)}}(k',k;q_1,\nu_1;q_2,\nu_2;q_3,\nu_3) = a^3\delta_{\nu_1,\nu_2}\delta_{\nu_2,\nu_3}\bar{\delta}_{4,\nu_1}\left(-\frac{4}{9}\sin[\frac{a}{2}(k'+k)_{\nu_1}]\right.$$
$$\left. +\frac{1}{6}\sin[a(k'+k+\frac{1}{2}q_1-\frac{1}{2}q_3)_{\nu_1}]\cos(\frac{a}{2}q_{2\nu_2}) + \frac{1}{18}\sin[a(k'+k)_{\nu_1}]\cos[\frac{a}{2}(k'-k)_{\nu_1}]\right).$$

Another important operator is the cloverleaf field strength tensor. Its Fourier transform is given by

$$
\begin{aligned}
&F_{\mu\nu}(k';k) = a^4 \sum_x e^{i(k'-k)\cdot x} F_{\mu\nu}(x) \\
&= \frac{i}{a} \sum_b \int d(k',k;q)\ [f^A_{\mu\nu}(q)\ \tilde{A}^b_\nu(q) - f^A_{\nu\mu}(q)\ \tilde{A}^b_\mu(q)]\ T^b \\
&+ ig \sum_{b_1 b_2} \int d(k',k;q_1,q_2)\ T^{b_1} T^{b_2} \Big\{ f^B_{\mu\nu}(q_1,q_2)\ \tilde{A}^{b_1}_\nu(q_1) \tilde{A}^{b_2}_\nu(q_2) \\
&- f^B_{\nu\mu}(q_1,q_2) \tilde{A}^{b_1}_\mu(q_1) \tilde{A}^{b_2}_\mu(q_2) + f^C_{\mu\nu}(q_1,q_2) \tilde{A}^{b_1}_\mu(q_1) \tilde{A}^{b_2}_\nu(q_2) - f^C_{\nu\mu}(q_1,q_2) \tilde{A}^{b_1}_\nu(q_1) \tilde{A}^{b_2}_\mu(q_2) \Big\} \\
&+ iag^2 \sum_{b_1 b_2 b_3} \int d(k',k;q_1,q_2,q_3)\ \left(T^{b_1} T^{b_2} T^{b_3} - \frac{1}{3} \mathrm{Tr} T^{b_1} T^{b_2} T^{b_3} \right) \\
&\Big\{ -f^F_{\mu\nu}(q_1,q_2,q_3)\ \tilde{A}^{b_1}_\nu(q_1) \tilde{A}^{b_2}_\mu(q_2) \tilde{A}^{b_3}_\nu(q_3) + f^D_{\mu\nu}(q_1,q_2,q_3)\ \tilde{A}^{b_1}_\mu(q_1) \tilde{A}^{b_2}_\mu(q_2) \tilde{A}^{b_3}_\mu(q_3) \\
&- f^D_{\nu\mu}(q_1,q_2,q_3)\ \tilde{A}^{b_1}_\nu(q_1) \tilde{A}^{b_2}_\nu(q_2) \tilde{A}^{b_3}_\nu(q_3) - f^E_{\nu\mu}(q_1,q_2,q_3)\ \tilde{A}^{b_1}_\mu(q_1) \tilde{A}^{b_2}_\mu(q_2) \tilde{A}^{b_3}_\nu(q_3) \\
&- f^E_{\nu\mu}(q_3,q_2,q_1)\ \tilde{A}^{b_1}_\nu(q_1) \tilde{A}^{b_2}_\mu(q_2) \tilde{A}^{b_3}_\mu(q_3) + f^E_{\mu\nu}(q_1,q_2,q_3)\ \tilde{A}^{b_1}_\nu(q_1) \tilde{A}^{b_2}_\mu(q_2) \tilde{A}^{b_3}_\mu(q_3) \\
&+ f^E_{\mu\nu}(q_3,q_2,q_1)\ \tilde{A}^{b_1}_\mu(q_1) \tilde{A}^{b_2}_\nu(q_2) \tilde{A}^{b_3}_\nu(q_3) + f^F_{\nu\mu}(q_1,q_2,q_3)\ \tilde{A}^{b_1}_\mu(q_1) \tilde{A}^{b_2}_\nu(q_2) \tilde{A}^{b_3}_\mu(q_3) \Big\} \\
&+ \mathcal{O}(g^3)
\end{aligned}
\tag{A7}
$$

where

$$
\begin{aligned}
f^A_{\mu\nu}(q) &= \sin(aq_\mu) \cos(\frac{a}{2} q_\nu), \\
f^B_{\mu\nu}(q_1,q_2) &= \cos[\frac{a}{2}(q_1+q_2)_\mu] \sin[\frac{a}{2}(q_1+q_2)_\nu] \sin[\frac{a}{2}(q_1-q_2)_\mu], \\
f^C_{\mu\nu}(q_1,q_2) &= \frac{1}{2}[\cos(\frac{a}{2}q_{1\mu}) \cos(aq_{1\nu} + \frac{a}{2}q_{2\nu}) + \cos(\frac{a}{2}q_{2\nu}) \cos(aq_{2\mu} + \frac{a}{2}q_{1\mu}) \\
&\quad + \cos(aq_{2\mu} + \frac{a}{2}q_{1\mu}) \cos(aq_{1\nu} + \frac{a}{2}q_{2\nu}) - \cos(\frac{a}{2}q_{1\mu}) \cos(\frac{a}{2}q_{2\nu})], \\
f^D_{\mu\nu}(q_1,q_2,q_3) &= \cos[\frac{a}{2}(q_1+q_2+q_3)_\mu] \Big\{ \frac{1}{6} \sin[a(q_1+q_2+q_3)_\nu] \\
&\quad - \cos[\frac{a}{2}(q_1+q_2+q_3)_\nu] \cos[\frac{a}{2}(q_1-q_3)_\nu] \sin(\frac{a}{2}q_{2\nu}) \Big\}, \\
f^E_{\mu\nu}(q_1,q_2,q_3) &= \cos[\frac{a}{2}(q_1+q_2+q_3)_\mu] \cos[\frac{a}{2}(q_1+q_2+q_3)_\nu] \cos[\frac{a}{2}(q_1+q_2)_\mu] \sin(\frac{a}{2}q_{3\nu}) \\
&\quad + \frac{1}{2} \cos[a(q_2 + \frac{1}{2}q_3)_\mu] \sin[\frac{a}{2}(q_1+q_2)_\nu], \\
f^F_{\mu\nu}(q_1,q_2,q_3) &= \cos[\frac{a}{2}(q_1+q_2+q_3)_\mu] \sin[a(\frac{1}{2}q_1 + q_2 + \frac{1}{2}q_3)_\nu] \cos[\frac{a}{2}(q_1-q_3)_\mu].
\end{aligned}
\tag{A8}
$$

Using $\tilde{A}^b_\mu(q)^* = \tilde{A}^b_\mu(-q)$, one can easily check that $F^b_{\mu\nu}(k';k)^* = F^b_{\mu\nu}(-k';-k)$. Furthermore, $F_{\mu\nu}(k';k) = -F_{\nu\mu}(k';k)$, as required. Note the absence of a $\mathrm{Tr} T^{b_1} T^{b_2}$ term

in the order g coefficient.

The Fourier transform of the improved cloverleaf field strength tensor has the same form as that for $F_{\mu\nu}$, but the functions $f^A_{\mu\nu}, \ldots$ must be replaced by the following functions:

$$\tilde{f}^A_{\mu\nu}(q) = \frac{1}{3}(5 - \cos(aq_\mu) - \cos(aq_\nu))f^A_{\mu\nu}(q),$$

$$\tilde{f}^B_{\mu\nu}(q_1,q_2) = \frac{1}{3}\Big\{(5 - \cos[a(q_1+q_2)_\mu] - \cos[a(q_1+q_2)_\nu])f^B_{\mu\nu}(q_1,q_2)$$
$$- \sin[a(q_1 + \frac{1}{2}q_2)_\nu]f^A_{\mu\nu}(q_1) + \sin[a(\frac{1}{2}q_1 + q_2)_\nu]f^A_{\mu\nu}(q_2)\Big\},$$

$$\tilde{f}^C_{\mu\nu}(q_1,q_2) = \frac{1}{3}\Big\{(5 - \cos[a(q_1+q_2)_\mu] - \cos[a(q_1+q_2)_\nu])f^C_{\mu\nu}(q_1,q_2)$$
$$+ \sin[a(q_1 + \frac{1}{2}q_2)_\nu]f^A_{\nu\mu}(q_1) + \sin[a(\frac{1}{2}q_1 + q_2)_\mu]f^A_{\mu\nu}(q_2)\Big\},$$

$$\tilde{f}^D_{\mu\nu}(q_1,q_2,q_3) = \frac{1}{3}\Big\{(5-\cos[a(q_1+q_2+q_3)_\mu]-\cos[a(q_1+q_2+q_3)_\nu])f^D_{\mu\nu}(q_1,q_2,q_3)$$
$$+ \sin[a(q_1 + q_2 + \frac{1}{2}q_3)_\mu]f^B_{\nu\mu}(q_1,q_2) - \sin[a(\frac{1}{2}q_1 + q_2 + q_3)_\mu]f^B_{\nu\mu}(q_2,q_3)$$
$$-\frac{1}{2}\cos[a(q_1 + \frac{1}{2}q_2 + \frac{1}{2}q_3)_\mu]f^A_{\nu\mu}(q_1) - \frac{1}{2}\cos[a(\frac{1}{2}q_1 + \frac{1}{2}q_2 + q_3)_\mu]f^A_{\nu\mu}(q_3)$$
$$+ \cos[a(\frac{1}{2}q_1 + q_2 + \frac{1}{2}q_3)_\mu]f^A_{\nu\mu}(q_2)\Big\},$$

$$\tilde{f}^E_{\mu\nu}(q_1,q_2,q_3) = \frac{1}{3}\Big\{(5-\cos[a(q_1+q_2+q_3)_\mu]-\cos[a(q_1+q_2+q_3)_\nu])f^E_{\mu\nu}(q_1,q_2,q_3)$$
$$- \sin[a(q_1 + q_2 + \frac{1}{2}q_3)_\mu]f^B_{\mu\nu}(q_1,q_2) - \sin[a(\frac{1}{2}q_1 + q_2 + q_3)_\nu]f^C_{\nu\mu}(q_2,q_3)$$
$$-\frac{1}{2}\cos[a(\frac{1}{2}q_1 + \frac{1}{2}q_2 + q_3)_\nu]f^A_{\nu\mu}(q_3)\Big\},$$

$$\tilde{f}^F_{\mu\nu}(q_1,q_2,q_3) = \frac{1}{3}\Big\{(5-\cos[a(q_1+q_2+q_3)_\mu]-\cos[a(q_1+q_2+q_3)_\nu])f^F_{\mu\nu}(q_1,q_2,q_3)$$
$$- \sin[a(q_1 + q_2 + \frac{1}{2}q_3)_\nu]f^C_{\nu\mu}(q_1,q_2) - \sin[a(\frac{1}{2}q_1 + q_2 + q_3)_\nu]f^C_{\mu\nu}(q_2,q_3)$$
$$- \cos[a(\frac{1}{2}q_1 + q_2 + \frac{1}{2}q_3)_\nu]f^A_{\nu\mu}(q_2)\Big\}. \qquad \text{(A9)}$$

REFERENCES

[1] B.A. Thacker and G. Peter Lepage, Phys. Rev. D **43**, 196 (1991).

[2] G. Peter Lepage, Lorenzo Magnea, Charles Nakhleh, Ulrika Magnea, and Kent Hornbostel, Phys. Rev. D **46**, 4052 (1992).

[3] C. T. H. Davies and B. A. Thacker, Phys. Rev. D **45**, 915 (1992).

[4] J. Mandula, G. Zweig, and J. Govaerts, Nucl. Phys. **B228**, 109 (1983).

[5] L.D. Faddeev and V.N. Popov, Phys. Lett. **25B**, 29 (1967).

[6] Hikaru Kawai, Ryuichi Nakayama, and Koichi Seo, Nucl. Phys. **B189**, 40 (1981).

[7] David G. Boulware, Ann. Phys. **56**, 140 (1970).

[8] G. Peter Lepage and Paul B. Mackenzie, NSF-ITP-90-227 (unpublished).

[9] M. Lüscher and P. Weisz, Nucl. Phys. **B266**, 309 (1986).

[10] Note that in terms of the parameters A, B, A_S, and Z defined in Ref. [3], the order g^2 corrections to the mass and wavefunction renormalization are given by $aA + B$ and $Z - aA_S$, respectively. See also Table II in Ref. [2].

TABLES

TABLE I. The energy shift parameter A for various values of the product of the bare heavy quark mass M and the lattice spacing a. The contribution to A from the quark-gluon loop diagram of Fig. 2(a) is denoted by $A_i(A)$ for the improved gluon action of Eq. (26) and by $A_s(A)$ for the simple gluon action of Eq. (24). The contribution from the tadpole diagram of Fig. 2(b) is denoted by $A_i(B)$ and $A_s(B)$ for the improved and simple gluon actions, respectively. For $aM \geq 2$, the stability parameter n is set to unity; for $1 \leq aM < 2$, $n = 2$ is used. Extrapolation uncertainties are no larger than ± 0.0001.

aM	$A_i(A)$	$A_i(B)$	$A_s(A)$	$A_s(B)$
5.00	0.0417	0.1361	0.0414	0.1688
4.75	0.0407	0.1387	0.0403	0.1719
4.50	0.0397	0.1415	0.0391	0.1754
4.25	0.0385	0.1446	0.0377	0.1793
4.00	0.0372	0.1480	0.0363	0.1835
3.75	0.0358	0.1519	0.0347	0.1883
3.50	0.0342	0.1562	0.0329	0.1937
3.25	0.0325	0.1611	0.0309	0.1998
3.00	0.0306	0.1667	0.0288	0.2067
2.75	0.0284	0.1732	0.0263	0.2147
2.50	0.0261	0.1807	0.0237	0.2241
2.25	0.0234	0.1896	0.0208	0.2351
2.00	0.0206	0.2002	0.0176	0.2482
1.90	0.0199	0.2046	0.0168	0.2536
1.80	0.0185	0.2101	0.0154	0.2603
1.70	0.0172	0.2160	0.0139	0.2677
1.60	0.0158	0.2226	0.0124	0.2759
1.50	0.0143	0.2300	0.0108	0.2850
1.40	0.0129	0.2383	0.0092	0.2952
1.30	0.0114	0.2476	0.0076	0.3068
1.20	0.0100	0.2584	0.0061	0.3201
1.10	0.0086	0.2708	0.0047	0.3354
1.00	0.0075	0.2850	0.0036	0.3530

TABLE II. The heavy quark mass renormalization parameter B for various values of the product of the bare heavy quark mass M and the lattice spacing a. The contribution to B from the quark-gluon loop diagram of Fig. 2(a) is denoted by $B_i(A)$ for the improved gluon action of Eq. (26) and by $B_s(A)$ for the simple gluon action of Eq. (24). The contribution from the tadpole diagram of Fig. 2(b) is denoted by $B_i(B)$ and $B_s(B)$ for the improved and simple gluon actions, respectively. For $aM \geq 2$, the stability parameter n is set to unity; for $1 \leq aM < 2$, $n = 2$ is used. Extrapolation uncertainties are no larger than ± 0.0001 for the tadpole values and ± 0.0002 for the contributions from the quark-gluon loop diagram.

aM	$B_i(A)$	$B_i(B)$	$B_s(A)$	$B_s(B)$
5.00	−0.0024	0.0556	−0.0030	0.0697
4.75	−0.0016	0.0568	−0.0021	0.0712
4.50	−0.0008	0.0582	−0.0011	0.0728
4.25	0.0000	0.0599	−0.0002	0.0748
4.00	0.0009	0.0619	0.0008	0.0771
3.75	0.0018	0.0642	0.0019	0.0798
3.50	0.0028	0.0670	0.0030	0.0832
3.25	0.0039	0.0704	0.0042	0.0872
3.00	0.0049	0.0747	0.0054	0.0923
2.75	0.0059	0.0801	0.0065	0.0987
2.50	0.0069	0.0871	0.0076	0.1070
2.25	0.0077	0.0963	0.0085	0.1181
2.00	0.0080	0.1091	0.0089	0.1334
1.90	0.0076	0.1175	0.0083	0.1438
1.80	0.0077	0.1248	0.0084	0.1525
1.70	0.0077	0.1332	0.0084	0.1626
1.60	0.0076	0.1431	0.0083	0.1746
1.50	0.0073	0.1550	0.0079	0.1889
1.40	0.0068	0.1692	0.0073	0.2061
1.30	0.0060	0.1868	0.0064	0.2274
1.20	0.0048	0.2089	0.0051	0.2541
1.10	0.0032	0.2373	0.0032	0.2885
1.00	0.0010	0.2752	0.0007	0.3345

TABLE III. The infrared-finite portion of the heavy quark wavefunction renormalization parameter C for various values of the product of the bare heavy quark mass M and the lattice spacing a. The infrared-finite contribution to C from the quark-gluon loop diagram of Fig. 2(a) is denoted by C_i for the improved gluon action of Eq. (26) and by C_s for the simple gluon action of Eq. (24). The tadpole diagram of Fig. 2(b) does not contribute to this parameter. For $aM \geq 2$, the stability parameter n is set to unity; for $1 \leq aM < 2$, $n = 2$ is used. Extrapolation uncertainties are no larger than ± 0.0001.

aM	C_i	C_s
5.00	0.0032	0.0029
4.75	0.0018	0.0014
4.50	0.0002	−0.0004
4.25	−0.0015	−0.0023
4.00	−0.0033	−0.0044
3.75	−0.0054	−0.0067
3.50	−0.0077	−0.0092
3.25	−0.0102	−0.0120
3.00	−0.0131	−0.0152
2.75	−0.0163	−0.0187
2.50	−0.0199	−0.0226
2.25	−0.0239	−0.0270
2.00	−0.0285	−0.0319
1.90	−0.0300	−0.0335
1.80	−0.0322	−0.0358
1.70	−0.0345	−0.0382
1.60	−0.0369	−0.0408
1.50	−0.0395	−0.0435
1.40	−0.0422	−0.0464
1.30	−0.0450	−0.0493
1.20	−0.0480	−0.0524
1.10	−0.0511	−0.0555
1.00	−0.0542	−0.0587

TABLE IV. Tadpole improvement of the energy shift parameter A and mass renormalization parameter B for various values of the product of the bare mass M and the lattice spacing a. Results are given for the simple gluon action only. The renormalization parameters without tadpole improvement are denoted by A_s and B_s; the improved parameters are denoted by $\tilde{A}_s$ and $\tilde{B}_s$. The perturbative value $u_0^{(2)} = -0.083$ is used for the mean-field parameter.

aM	A_s	$\tilde{A}_s$	B_s	$\tilde{B}_s$
5.00	0.210	0.069	0.067	0.006
4.00	0.220	0.064	0.078	0.012
3.00	0.236	0.056	0.098	0.022
2.00	0.266	0.038	0.142	0.035
1.70	0.282	0.028	0.171	0.036
1.30	0.314	0.008	0.234	0.039
1.00	0.357	−0.017	0.335	0.041

FIGURES

FIG. 1. Various Feynman diagram elements. A curly line represents a gluon; a double solid line indicates a heavy quark. (a) Heavy quark propagator; (b) gluon propagator; (c) lowest-order vertices involving a heavy quark line and r gluons; (d) the $O(g^2)$ counterterm from link variable renormalization.

FIG. 2. Two Feynman diagrams which contribute to the heavy quark self-energy. A curly line denotes a gluon; a double solid line denotes a heavy quark.

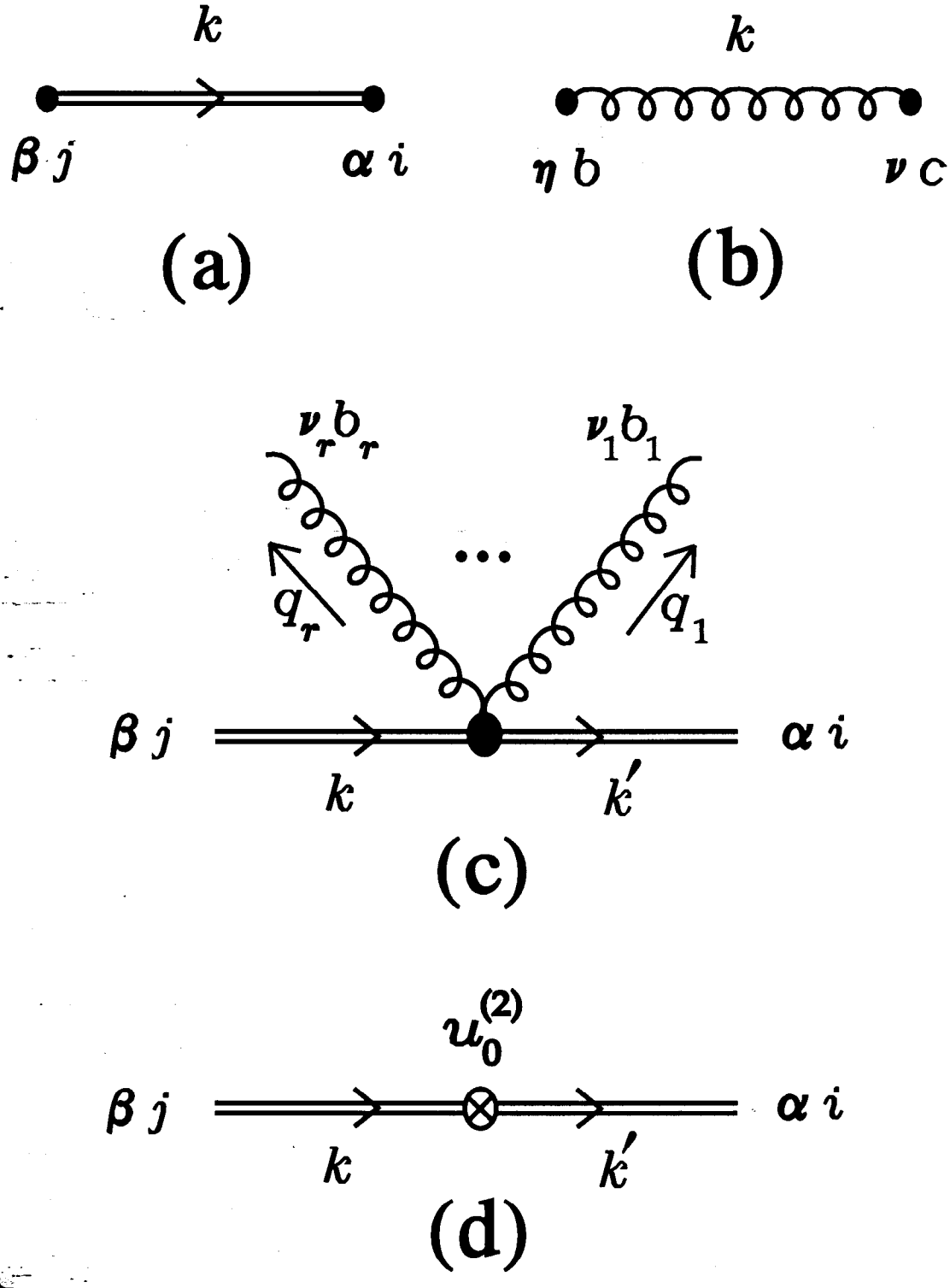

Figure 1

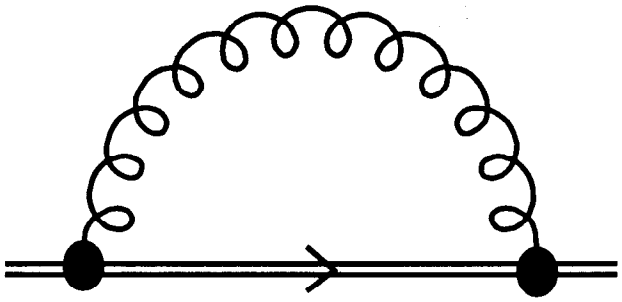

(a)

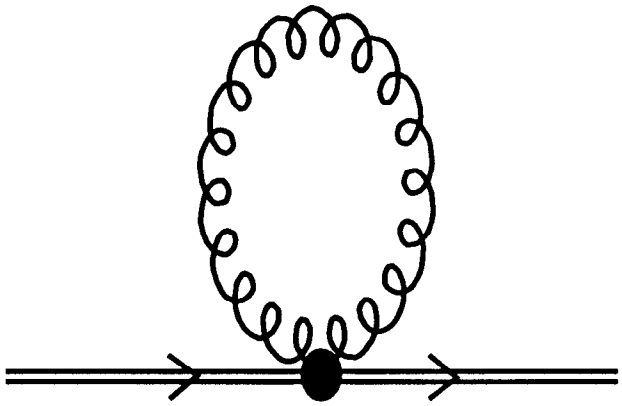

(b)

Figure 2